Stage-Dependent Inhibition of HIV-1 Replication by Antiretroviral Drugs in Cell Culture[▽]

Daniel A. Donahue,[1,2] Richard D. Sloan,[1] Björn D. Kuhl,[1,3] Tamara Bar-Magen,[1]
Susan M. Schader,[1,2] and Mark A. Wainberg[1,2,3]*

*McGill University AIDS Centre, Lady Davis Institute, Jewish General Hospital, Montréal, Quebec, Canada[1]; Department of
Microbiology and Immunology, McGill University, Montréal, Quebec, Canada[2]; and Department of Experimental Medicine,
McGill University, Montréal, Quebec, Canada[3]*

Recent clinical trials have shown that the use of the HIV-1 integrase (IN) inhibitor raltegravir (RAL) results in drops in the viral load that are more rapid than those achieved by use of the reverse transcriptase (RT) inhibitor efavirenz. Previously, mathematical modeling of viral load decay that takes into account the stage of viral replication targeted by a drug has yielded data that closely approximate the clinical trial results. This model predicts greater inhibition of viral replication by drugs that act later in the viral replication cycle. In the present study, we have added drugs that target entry, reverse transcription, integration, or proteolytic processing to acutely infected cells and have shown modest viral inhibition by entry inhibitors, intermediate levels of inhibition by RT and IN inhibitors, and high levels of inhibition by protease inhibitors relative to the levels of growth for the no-drug controls. When dual or triple combinations of these drugs were added to acutely infected cells, we found that the levels of inhibition achieved by any given combination were comparable to those achieved by the latest-acting drug in the combination. In single-round infections in which the kinetics of reverse transcription and integration had been determined by quantitative PCR, addition of IN inhibitors at various times postinfection resulted in levels of inhibition equal to or greater than those achieved by addition of RT inhibitors. Collectively, our data provide *in vitro* evidence of the stage-dependent inhibition of HIV-1 by clinically relevant drugs. We discuss how stage-dependent inhibition helps to explain the unique viral load decay dynamics observed clinically with RAL.

Upon the initiation of highly active antiretroviral therapy (HAART) for the treatment of HIV infection, the level of viral RNA in the blood rapidly decays in at least two distinct phases (12, 28), according to the death rates of cells that were already infected before treatment began. First-phase decay occurs during the first 7 to 10 days of treatment and has a half-life of 0.9 to 1.6 days (6, 28, 29), reflecting the death rate of productively infected CD4^{+} T cells. The slower second phase occurs over a period of weeks and exhibits a half-life of approximately 14 days (28), corresponding to the turnover rate of long-lived infected cells. Second-phase sources of virus are believed to include cells of the monocyte/macrophage lineage and may also include infected resting CD4^{+} T cells carrying unintegrated DNA (preintegration latent cells), follicular dendritic cells harboring intact virions, infected CD4^{+} T cells that are not cleared by the host immune response, and an as-yet-unidentified cell type (4, 12, 17, 28, 30). An extremely slow third phase of decay is detectable by more sensitive assays and has a half-life estimated to range from months to years (7, 11). The viremia in this phase is believed to result from the reactivation of latently infected CD4^{+} T cells (11, 40) or low-level ongoing replication (8, 14, 32), or both (35).

Recent clinical trials with the first clinically approved HIV-1 integrase (IN) inhibitor, raltegravir (RAL), have yielded promising results. The phase II Merck protocol 004 part II trial (22, 23) and the phase III STARTMRK trial (20) compared the activity of RAL to that of the nonnucleoside reverse transcriptase inhibitor (NNRTI) efavirenz (EFV), each as part of standard combination therapy in drug-naïve HIV-1-infected individuals. While both drugs showed equal efficacy for the long-term suppression of the viral load, the limit of detection was reached more rapidly with RAL. This has been attributed to levels of virus production from second-phase sources that were 70% lower with RAL-based treatment than with EFV-based treatment (26).

Several hypotheses may explain these unique viral load decay dynamics. They include differences in the time until drug bioavailability, differences in drug potency, a role for cells latently infected preintegration, the greater penetration of certain drugs into sanctuary sites, the stage of viral replication targeted, and the IN inhibitor-induced accumulation of unintegrated viral DNA (15, 23, 26, 33, 34). On the basis of the mathematical modeling of viral load decay, it has been proposed that the clinical observations can be explained by the effect of RAL on cells latently infected preintegration (26). These models also suggest that differences in drug potency might play a minor role but are inconsistent with a role for sanctuary sites (26). The mathematical models of viral load decay prepared by others suggest that the stage of viral replication targeted by RAL versus that targeted by EFV can explain the clinical trial results but are inconsistent with roles for cells latently infected preintegration, differences in drug potency or the time until bioavailability, or sanctuary sites (33, 34). Furthermore, the latter models involving cells latently

* Corresponding author. Mailing address: McGill University AIDS Centre, Lady Davis Institute, Jewish General Hospital, Montréal, QC H3T 1E2, Canada. Phone: (514) 340-8222, ext. 5282. Fax: (514) 340-7537. E-mail: mark.wainberg@mcgill.ca.

infected preintegration used parameters based on the experimentally determined kinetics of reverse transcription, integration, and preintegration complex decay during infection of resting CD4$^+$ T cells (19, 31, 45) and strongly argue that the action of RAL in this cell type cannot account for the clinical trial observations (34). This is in contrast to the parameter choices concerning cells latently infected preintegration used previously (26), which are in conflict with the known properties of this viral reservoir. Others have suggested that the greater decay observed with RAL could be a result of the gene expression from or the apoptosis triggered by unintegrated DNA that accumulates following the use of an IN inhibitor (15). However, these effects would occur in cells that are unable to produce virus (since productive infection has been blocked by the IN inhibitor) and therefore would not be expected to contribute to the viral load, although the possibility that these effects play a role in superinfected cells cannot be excluded. Given that the outputs of certain mathematical models of viral load decay (33, 34) have closely approximated the clinical trial results, it seems probable that the stage of viral replication targeted by RAL versus that targeted by EFV may help to explain the viral load decay dynamics observed.

The mathematical model of stage-dependent inhibition of viral replication is detailed elsewhere (33, 34) but can be summarized as follows. Large numbers of virions are produced only by cells that were infected prior to the start of treatment (since the majority of active viral replication is immediately blocked following the initiation of HAART [10, 37]), and virus production from these cells lasts until their death, implying that the viral load decays according to the death of previously infected cells. Two factors that affect the decay of viremia can differ depending on the stage of viral replication targeted by a drug and the cell type in which the drug is acting. These factors are (i) the death rates of the virus-producing cells and (ii) the time of transition from early- to late-stage-infected (i.e., virus-producing) cells. This model predicts that the most rapid decay of virus production should result from the use of drugs targeting the latest stages of viral replication. This concept can also be presented in terms of the number of cells available to a given drug when treatment begins. At the time of drug addition, drugs that act at a later stage of replication, such as integration or proteolytic processing, will have more available target cells in which to prevent viral replication than drugs that act earlier, such as at entry or reverse transcription. This is because some viruses will have completed the earlier but not the later stages of replication during ongoing infection, such that a later-stage inhibitor can block most or all of these viruses, while the earlier-stage inhibitor cannot be effective beyond the early stage of replication that it targets. Importantly, this model applies to infection of any cell type, including those responsible for either first-phase decay (productively infected CD4$^+$ T cells) or second-phase decay (e.g., macrophages) and can be used to analyze either phase individually or both phases together. Since productively infected CD4$^+$ T cells are rapidly cleared (by cytopathic effect or CD8$^+$-mediated killing) but long-lived infected cells such as macrophages can produce virus over the remainder of their lifetimes, the influence of the stage effect on viremia should have a greater duration in the second phase. While this hypothesis is supported by mathematical modeling, it has not been examined *in vitro*. Our study

was carried out to examine this hypothesis in cell culture in order to better understand the results obtained in clinical trials with RAL.

(The work by D.A.D. was performed in partial fulfillment of the requirements for a Ph.D. degree from the Faculty of Graduate Studies and Research, McGill University, Montréal, Québec, Canada.)

MATERIALS AND METHODS

Cells and viruses. PM1 cells (21) and SupT1 cells (38) were obtained through the NIH AIDS Research and Reference Reagent Program. PM1 and SupT1 cells were maintained in RPMI 1640 medium (Invitrogen), and 293T cells were maintained in Dulbecco modified Eagle medium (Invitrogen), each of which was supplemented with 10% fetal bovine serum, 1% L-glutamine, and 1% penicillin-streptomycin. The viral constructs pNL4-3 (1), pNL4-3(AD8) (13), and pNL4-3-deltaE-EGFP (where EGFP is enhanced green fluorescent protein) (44) (courtesy of R. Siliciano) were obtained through the NIH AIDS Research and Reference Reagent Program. pVPack-VSV-G (Stratagene), which encodes the vesicular stomatitis virus (VSV) envelope glycoprotein, was used to produce VSVg-pseudotyped NL4-3-deltaE-EGFP. The envelope sequence of pNL4-3(AD8) (GenBank accession number AF004394) was cloned into pcDNA3.1 (Invitrogen) and was used to produce AD8env-pseudotyped NL4-3-deltaE-EGFP. All transfections were performed in 293T cells with Lipofectamine 2000 (Invitrogen). Forty-eight hours after transfection, the viruses were treated with 100 U/ml DNase I (Invitrogen) in the presence of 10 mM MgCl$_2$ (added) for 1 h at 37°C to digest contaminating plasmid DNA, prior to filtration through a 0.2-μm-pore-size filter and storage at −80°C.

Antiviral compounds. AMD3100 (a CXCR4 coreceptor antagonist), darunavir (DRV), enfuvirtide (T-20), and nevirapine (NVP) were obtained through the NIH AIDS Research and Reference Reagent Program. EFV was a gift from Bristol-Myers Squibb Inc. Elvitegravir (EVG; an IN inhibitor), emtricitabine (FTC), and tenofovir disoproxil fumarate (TDF) were gifts from Gilead Sciences, Inc. Lopinavir (LPV) was a gift from Abbott Laboratories. MK-2048 (an IN inhibitor) and RAL were gifts from Merck-Frosst Canada, Inc.

Cell culture model to test stage-dependent inhibition of viral replication. PM1 cells (0.125 × 10^6) were infected with 18 ng p24 NL4-3 in T-25 flasks in 10 ml RPMI 1640 medium by adding virus and gently mixing the components without washing off the virus. Four days later, duplicate flasks of infected cells were pooled and the cells were seeded into 96-well plates at 190 μl per well. Uninfected cells were similarly grown to the same density before they were seeded into 96-well plates. Twenty-four hours after seeding of the plates, 10 μl of drug was added to replicate wells (to concentrations that could block virus replication by close to 100%, as determined in preliminary experiments in which the cells were pretreated with drug 1 h prior to infection). At 24 h following addition of drug, supernatants were collected to quantify the p24 antigen level by enzyme-linked immunosorbent assay (ELISA) or to quantify the viral RNA load by quantitative reverse transcriptase PCR (qRT-PCR). At no point were the cells split or was the virus washed from the wells. The final drug concentrations were as follows: T-20, 250 nM; AMD3100 and DRV, 1 μM; FTC and NVP, 10 μM; TDF, 100 μM; EFV, RAL, MK-2048, and EVG, 500 nM; and LPV, 5 μM. When they were used in combinations, each drug was used at the same concentration indicated above.

Single-round infections and flow cytometry. PM1 cells were infected with 576 ng p24 AD8env-pseudotyped NL4-3-deltaE-EGFP per 10^6 cells, and SupT1 cells were infected with 12 ng p24 VSVg-pseudotyped NL4-3-deltaE-EGFP per 10^6 cells, each by spinoculation for 2 h at 1,200 × g at 25°C, as described previously (27). Pseudotyped viruses were used to ensure that all viral DNA quantified by quantitative PCR (qPCR) was derived from a single round of replication. The start of spinoculation denotes the start of infection. For determination of the viral replication kinetics by qPCR, infected PM1 cells were used. Cells were washed three times with RPMI 1640 medium immediately following spinoculation to remove unbound virus and were resuspended in RPMI 1640 medium. The cells were collected at various times postinfection (p.i.) and stored at −80°C. Mock infections with heat-inactivated virus were carried out to quantify any residual plasmid DNA from transfection. For flow cytometry-based experiments, both infected PM1 cells and infected SupT1 cells were used (in separate experiments). Drug addition time courses were performed by addition of individual drugs to different wells of infected cells at different times. For drug addition at time zero (immediately prior to the start of spinoculation), RAL, MK-2048, EFV, or NVP was individually added at a concentration that was ≥99.5% the

inhibitory concentration (as determined in preliminary experiments), while the remaining wells contained RPMI 1640 medium only. Spinoculation was then performed as described above. The cells were washed three times with RPMI 1640 medium immediately, following spinoculation to remove unbound virus, and were then resuspended in RPMI 1640 medium with drug (time zero wells) or without drug (all other wells). For other drug addition time points, RAL, MK-2048, EFV, or NVP was added to individual wells. At 48 h p.i., the cells were fixed in 1% paraformaldehyde for 20 min. Flow cytometry was performed with a FACSCalibur instrument (Becton Dickinson) by gating for live cells and quantifying the number of cells positive for the expression of the virally encoded green fluorescent protein (GFP), and the data were analyzed with CellQuest Pro software.

qRT-PCR for viral RNA and qPCR for viral DNA. (i) Viral RNA. Viral RNA was extracted from the supernatants of infected cells by using a QIAamp viral RNA minikit (Qiagen). RT-PCR was performed with a Superscript III Platinum one-step qRT-PCR kit (Invitrogen) on a Corbett Rotor-Gene 6000 thermocycler. Dually labeled probes for this and all reactions described below were obtained from Biosearch Technologies (Novato, CA). The cycling conditions were 50°C for 15 min, 95°C for 8 min, and 45 cycles at 95°C for 15 s and 60°C for 30 s. The primers and probe used were primer total F, primer total R, and total probe (42). Reactions carried out in the absence of reverse transcriptase (Platinum *Taq* only) confirmed the absence of contaminating DNA. The samples were quantified against cloned standards.

(ii) Early and late reverse transcripts and 2-LTR circles. Cellular DNA was extracted with a DNeasy blood and tissue kit (Qiagen). PCR was performed with Platinum qPCR SuperMix-UDG (Invitrogen) on a Corbett Rotor-Gene 6000 thermocycler. The samples were normalized for their beta-globin contents and quantified against cloned standards that were diluted with DNA from uninfected cells. The cycling conditions were 50°C for 2 min, 95°C for 1 min, and 45 cycles at 95°C for 3 s and 60°C for 30 s, with 65 ng template being used per reaction mixture. The primers and probes used for the early reverse transcripts were primers ERT2F and ERT2R (25) and probe ERT (5′–6-carboxyfluorescein [FAM]–ACTAGAGATCCCTCAGACCCTTTT–BHQ1–3′. For the late reverse transcripts, primer total F, primer total R, and total probe were used (42). For 2-long terminal repeat (2-LTR) circles, primer circle F, primer circle R, and circle probe were used (42). For beta-globin, primer BetaGlo-F (5′-GGTACG GCTGTCATCACTTAGAC-3′), primer BetaGlo-R (5-AACGGCAGACTTCT CCTCAG-3′), and the BetaGlo-probe (5′-FAM-CTCACCCTGTGGAGCCAC ACC-BHQ1-3′) were used.

(iii) Integrated DNA. DNA was extracted and normalized as described above. A previously described Alu-*gag* PCR (43) was used with the following modifications. The first-round reaction was performed with undiluted samples (65 ng template) and 1:10 dilutions of each sample (6.5 ng template diluted with uninfected DNA, 65 ng DNA total) in the presence of 2 mM $MgCl_2$ and 200 µM deoxynucleoside triphosphates (dNTPs). Nine microliters of the resulting first-round product was used as the template for the second round of the nested reaction in the presence of 5 mM $MgCl_2$ (final concentration, including the carryover from first round) and 200 µM dNTPs was added; only the wild-type probe was used (43). The second-round cycling conditions were as described above for the 2-LTR circles. To generate a standard curve for the relative quantification of integrated DNA, the Alu-*gag* PCR was first performed with a dilution series of DNA from infected PM1 cells (diluted with DNA from uninfected cells).

Statistical analyses. Unpaired two-tailed *t* tests were used to test for statistically significant differences between each treatment group and the no-drug control group (see Fig. 2) and for differences between the amounts of p24 or viral RNA measured (see Fig. 4). One-way analysis of variance (ANOVA) was used to test for statistically significant differences within treatment groups (see Fig. 3). When such differences were found ($P < 0.05$), Dunnett's multiple-comparison test was used to test for statistically significant differences between the activity of the treatment with a single drug and the activity of a drug combination. All statistical analyses were performed with GraphPad Prism (version 4.0) software.

RESULTS

Establishment of a cell culture model of stage-dependent inhibition of HIV-1 replication. To test the concept of stage-dependent inhibition of virus replication *in vitro*, we established a cell culture model of ongoing infection using the PM1 cell line (Fig. 1A). Initial experiments were performed to determine the growth and infection conditions that would meet
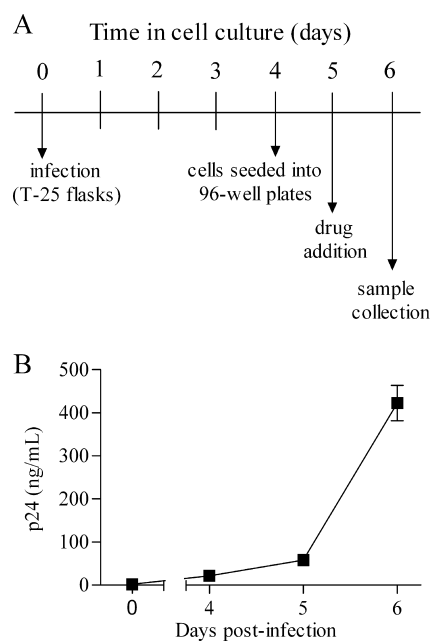

FIG. 1. Cell culture model of ongoing infection to test stage-dependent inhibition of HIV-1 replication. (A) Schematic representation of the experimental approach used to test stage-dependent inhibition of HIV-1 *in vitro*. PM1 cells were infected in bulk with NL4-3 and seeded into 96-well plates 4 days later to ensure that all wells contained cells that produced approximately the same amount of replicating virus. (B) Progress of infection over the course of 6 days in the absence of drug. The results depict the mean ± standard error of the mean from one experiment performed in triplicate and are representative of the results of three independent experiments.

two criteria: (i) infection would be ongoing for several days, without the washing off of newly produced virus, to ensure the simultaneous presence of viruses at various stages of replication; and (ii) the levels of virus production would be sufficient for quantification while remaining low enough after several days of infection to avoid excessive cytopathic effects. Thus, infection of PM1 cells with NL4-3 was allowed to proceed for 5 days prior to the addition of different drugs, and the supernatants were collected 24 h after drug addition. Since the drug concentrations used were such that close to 100% inhibition of replication could be achieved by any drug alone, any virus release between days 5 and 6 should result only from cells in which virus replication by day 5 (the time of drug addition) had progressed beyond the stage of replication targeted by the particular drug that had been used. In our system, most virus production (in the absence of drug) occurred between days 5 and 6 (Fig. 1B). Therefore, the amount of virus present on day 6 (24 h after drug addition) can be used to determine the stage-dependent effect that different inhibitors might have on virus production. Since high drug levels were present at the time of sample collection, we could not use either reverse transcriptase or infectivity assays to measure virus production. Similarly, measurement of viral RNA levels would be impractical since the viral RNA can still be produced in the presence of protease (PR) inhibitors. Therefore, we assayed for the presence of processed, extracellular p24 antigen as a measurement of virus production.

TABLE 1. Drugs used in this study[a]

Drugs used individually				Drug used in combination	
Entry inhibitors	RT inhibitors	IN inhibitors	PR inhibitors	Dual combinations	Triple combinations
AMD3100	TDF	RAL	LPV	EFV + AMD3100	EFV + TDF + FTC
T-20	FTC	MK-2048	DRV	RAL + AMD3100	RAL + TDF + FTC
	NVP	EVG		RAL + EFV	DRV + TDF + FTC
	EFV			DRV + AMD3100	
				DRV + EFV	
				DRV + RAL	

[a] The drug names, abbreviations, and concentrations used are given in Materials and Methods.

Later-acting drugs inhibit virus production to a greater extent than earlier-acting drugs when they are added during ongoing infection. We investigated four different stages of viral replication, i.e., entry, reverse transcription, integration, and proteolytic processing, using two or more drugs that act at each of these stages (Table 1). Drugs were added individually after 5 days of infection, and the amount of p24 antigen present at day 6 was determined. The results presented in Fig. 2 show that the drugs that target the latest steps of the viral replication cycle (i.e., PR inhibitors) inhibited virus production to a greater extent than the drugs that act at earlier stages (i.e., entry inhibitors), although the NNRTIs EFV and NVP inhibited virus production at least as well as the other RT and IN inhibitors that were employed. The greater inhibition by EFV can likely be attributed to previously reported pharmacological slope parameters (36), as discussed below.
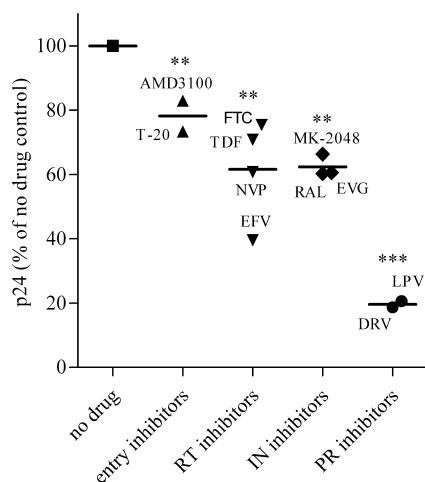

FIG. 2. Stage-dependent inhibition of HIV-1 replication by individual drugs. Infection of PM1 cells with NL4-3 and drug treatments were carried out as described in the legend to Fig. 1. For each of four stages of viral replication, two or more drugs were individually added during ongoing replication at 5 days after infection. p24 measurements were performed with samples collected 6 days after infection (1 day after drug addition). Each data point represents, for any given drug, the average of the means of three independent experiments, each of which was performed in duplicate or triplicate wells, relative to the results for the no-drug controls. Horizontal lines represent the averages of the means of all drugs targeting that stage of replication. Unpaired two-tailed t tests were used to test for statistically significant differences between the no-drug controls and each treatment group. For no drug versus entry inhibitors, $P = 0.0061$; for no drug versus RT inhibitors, $P = 0.0059$; for no drug versus IN inhibitors, $P = 0.0021$; for no drug versus PR inhibitors, $P < 0.0001$.

The latest-acting drug in a combination largely determines the level of inhibition of viral replication when it is added during ongoing infection. We next looked at the effects of drug combinations to determine whether, as predicted (33), the latest-acting drug in a combination would dictate the level of inhibition of viral replication. In the same manner as that used for the individual drugs, dual- or triple-drug combinations were added to cells that had been infected for 5 days (Table 1). Dual-drug combinations were selected such that each pair of different-stage inhibitors would be employed, while triple-drug combinations were selected by taking into account both the findings of the clinical trials comparing RAL and EFV (20, 22, 23) and the current first-line treatment recommendations in the United States (16). The results presented in Fig. 3 show that the addition of an earlier-acting drug to a later-acting drug resulted in levels of inhibition similar to that obtained by using the later-acting drug alone. One-way ANOVA showed that when an RT or PR inhibitor was the latest-acting drug in a combination, there was no statistically significant difference in the amount of viral inhibition compared to that achieved by the use of the RT or PR inhibitor alone. However, one-way ANOVA showed that there was a statistically significant difference ($P = 0.021$) in the responses within the group when an IN inhibitor was the latest-acting drug. A subsequent Dunnett's multiple-comparison test (a posttest used after an ANOVA that looks for differences between control and treatment groups, which, in this case, are the differences between the use of RAL alone and in a combination as the latest-acting drug) showed that the addition of EFV as an earlier-acting drug resulted in greater inhibition ($P < 0.05$) than the use of RAL alone, which is consistent with the results reported in Fig. 2 and which is likely attributable to pharmacological slope parameters, as discussed below. In contrast, there were no significant differences in inhibition between that achieved when other earlier-acting drugs were added to RAL and that achieved by the use of RAL alone.

Measurement of viral RNA masks the antiviral activity achieved by PR inhibitors following drug addition but not that achieved by other drug classes. The model of stage-dependent inhibition of viral replication predicts that drugs acting the latest in the viral replication cycle will result in the greatest level of decay of viremia (33), and our results are consistent with that prediction (Fig. 2 and 3). However, clinical trials with RAL showed more rapid drops in viral load than had previously been shown for other drugs, including PR inhibitors, which act at a later stage of replication than IN inhibitors. We therefore wished to determine whether this apparent discrep-
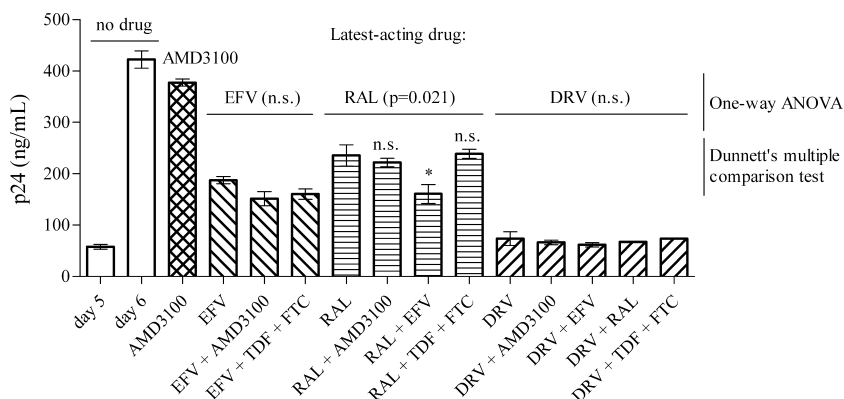
FIG. 3. Stage-dependent inhibition of HIV-1 replication by drug combinations. Infection of PM1 cells with NL4-3 and drug treatments were carried out as described in the legend to Fig. 1. Individual drugs or drug combinations were added during ongoing replication at 5 days after infection. p24 measurements were performed with samples collected 6 days after infection (1 day after drug addition). Drug combinations are grouped according to the drug that acts the latest in the viral replication cycle (for example, the combination of an IN inhibitor and an entry inhibitor is in the IN inhibitor group, while the combination of an IN inhibitor and a PR inhibitor is in the PR inhibitor group). Data are expressed as the means ± standard errors of the means of one experiment performed in triplicate and are representative of the results of three independent experiments. For each of the three latest-acting drug combination groups (RT, IN, or PR inhibitors), one-way ANOVA was used to test for statistically significant differences in p24 levels within each group. When one-way ANOVA indicated that P was <0.05, which was observed only for the IN inhibitor (RAL) group, Dunnett's multiple-comparison test was performed. This was used to test for statistically significant differences between the single drug (RAL) and all combinations in which RAL was the latest-acting drug used to identify whether the activity of any combination(s) differed significantly from that of the RAL-only treatment. n.s., not significant; *, $P < 0.05$.

ancy might be due to measurement of the viral load as a marker of drug efficacy, as opposed to measurement of a viral product whose production is blocked by PR inhibitors (such as processed p24). In experiments similar to those whose results are presented in Fig. 1 to 3, all drugs listed in Table 1 were added individually to acutely infected PM1 cells at 5 days p.i., and the levels of p24 and viral RNA in supernatants collected at 24 h after drug addition were determined. The results presented in Fig. 4 show that the measurements of p24 or viral RNA were comparable in tests with all drugs acting prior to proteolytic processing. Conversely, the use of PR inhibitors led to very low levels of processed p24 compared to the levels for the no-drug controls, although the levels of viral RNA present after the use of PR inhibitors were significantly higher than those for the other drugs used.

Stage-dependent inhibition during single-round infection. To complement the results presented above, we also wished to study a pseudovirus capable of only a single round of infection. This would allow us to determine whether stage effects might occur in a more tightly controlled system, in which the levels of inhibition might be correlated to the stage of viral replication that was under way at the time of drug addition.

First, qPCR was used to determine the replication kinetics of a GFP-encoding NL4-3-based pseudovirus following the synchronous infection of PM1 cells. The early and late reverse transcription products, 2-LTR circles, and integrated DNA were quantified (Fig. 5A and B); and from those quantities we determined the time points for drug addition in further experiments. Next, we added the RT inhibitor EFV or NVP or the IN inhibitor RAL or MK-2048 at defined time points after infection of PM1 cells by the same virus. The percentage of GFP-positive cells was measured by flow cytometry at 48 h p.i. (Fig. 5C). Our data show that over time the use of IN inhibitors
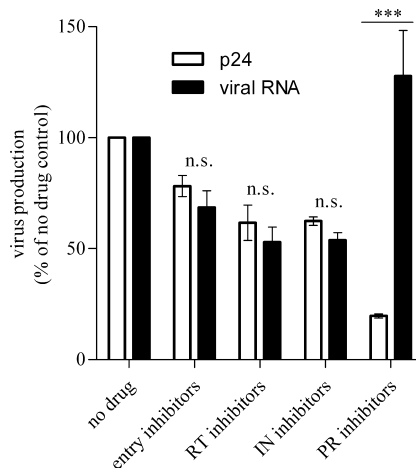

FIG. 4. Comparison of p24 and viral RNA levels as markers for the antiviral activities of drugs acting at different stages of HIV-1 replication. Infection of PM1 cells with NL4-3 and drug treatments were carried out as described in the legend to Fig. 1. For each of four different stages of viral replication, two or more drugs were individually added during ongoing replication at 5 days after infection (all drugs listed in Table 1 were used individually). Measurements of p24 (by ELISA) or viral RNA (by qRT-PCR) levels were performed with samples collected 6 days after infection (1 day after drug addition). Each bar represents the mean inhibition of virus production relative to that for the no-drug controls for all drugs acting at a particular stage of replication (Table 1); average values for each drug were calculated from the means of three independent experiments, each of which was performed in replicate wells. Error bars represent standard errors of the means. Unpaired two-tailed t tests were used to test for statistically significant differences between measurements of p24 or viral RNA as an indicator of inhibition of virus replication for each class of drug. n.s., not significant; ***, $P < 0.0001$.
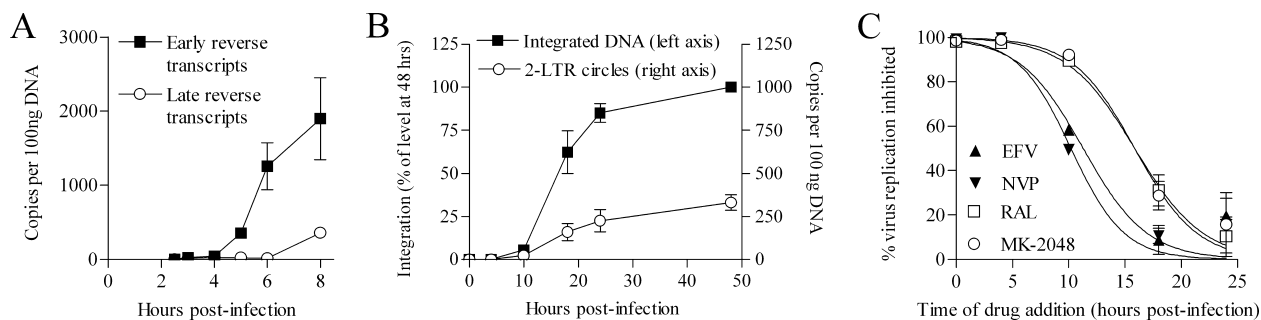
FIG. 5. Kinetics of reverse transcription, integration, and stage-dependent inhibition of HIV-1 replication during single-round infections. PM1 cells were infected by spinoculation with NL4-3-deltaE-EGFP pseudotyped with the AD8 envelope (capable of only a single round of infection) and washed extensively to remove unbound virus. Early and late reverse transcription products (A) and integrated DNA and 2-LTR circles (B) were quantified by qPCR. (C) The RT inhibitor EFV or NVP or the IN inhibitor RAL or MK-2048 was added individually at defined time points after infection of PM1 cells by the same virus. The percentage of GFP-positive cells was determined at 48 h p.i. by flow cytometry and is expressed relative to that for the no-drug control. Data represent the means ± standard errors of the means of three independent experiments and were fitted to sigmoidal dose-response (variable slope) curves.

consistently resulted in the inhibition of viral replication at levels equal to or greater than those achieved with RT inhibitors when they were added at discrete time points following single-round infection. Similar results were obtained when these experiments were repeated with SupT1 cells (data not shown).

DISCUSSION

The continuous evolution of drug-resistant variants of HIV-1 and HIV-2, combined with the adverse effects and the toxicity associated with many available drugs, necessitates the ongoing development of novel antiretrovirals with nonoverlapping resistance profiles and improved tolerance. RAL represents a major step forward in this regard since it is the first in a new class of drugs, has fewer reported adverse effects than EFV (22, 23), and appears to have achieved better initial results as part of first-line combination therapy than one of the most successful regimens currently available. The most plausible explanation reported in the literature to help interpret the unique viral load decay dynamics observed with RAL comes from mathematical modeling of the stage-dependent inhibition of viral replication (33, 34).

In the present study, we wished to establish a cell culture model of stage-dependent inhibition of viral replication that would provide *in vitro* evidence to support or counter the predictions made by mathematical modeling of the stage effect. Since this model applies to both first- and second-phase sources of virus and can be used to analyze either phase of decay separately but since the cells responsible for second-phase virus production remain to be conclusively identified (4, 17, 34), we decided to use a cell line that represents a first-phase source of virus production. Additionally, we reasoned that if our data provided evidence for stage-dependent inhibition in a first-phase source such as T cells, this would add strength to the application of this concept to additional (second-phase) sources.

We first described a cell culture model of ongoing infection in which drug is added after several days of infection, such that viruses at various stages of replication are represented simultaneously (Fig. 1). The infection conditions in this model per-

mit the detection of p24 levels at 1 day after drug addition to determine whether stage effects might occur *in vitro*. When drugs targeting one of four different stages of viral replication were added individually to infected cells, we observed that the levels of inhibition achieved were, in general, strongly influenced by the stage of viral replication targeted (Fig. 2). We next showed that the latest-acting drug in a combination largely determined the extent of inhibition achieved, since the addition of one or more earlier-acting drugs to a later-acting drug generally resulted in little additional effect (Fig. 3).

We then showed that measurement of viral RNA rather than another marker of virus production (i.e., processed p24) masks the antiviral activity that is achieved by PR inhibitors but not by inhibitors of other stages of viral replication following drug addition. (Fig. 4). This is an expected result, since viral RNA is still produced in the presence of PR inhibitors and likely explains the apparent discrepancy between the greater antiviral effect that late-acting drugs are predicted to have (33) and clinical observations that the use of RAL achieves a decay in the level of viremia more rapid than that which had been observed with all other drugs. Finally, we performed infections with viruses capable of only a single round of replication; in those experiments, we had already determined the kinetics of reverse transcription and integration. Levels of inhibition by the later-acting drugs equal to or greater than the levels of inhibition by earlier-acting drugs were observed when drugs were added at any time point up to the time that the latest stage of replication targeted was mostly complete (Fig. 5). Taken together, our data represent the first *in vitro* evidence that the stage of viral replication targeted by a class of drug during ongoing infection contributes to the level of viral inhibition initially achieved by that drug.

It is notable that EFV achieved a greater level of inhibition than other RT or IN inhibitors in our ongoing-infection experiments but not in the single-round-infection experiments, a deviation from the overall trend of the stage-dependent inhibition of viral replication. This highlights the fact that additional factors, including pharmacological differences between individual drugs, likely also contribute to the levels of viral inhibition that are achieved. The results achieved with EFV in particular may be attributable to its reported ability to achieve

very high levels of inhibition at each round of viral replication, as illustrated by pharmacological parameters related to the slope of a drug's dose-response curve (36). Our experiments were designed to determine whether or not stage effects occur in general when the activities of drugs that target different stages of replication are compared and not to make direct comparisons of the activities of any two drugs. Furthermore, our data show that stage-dependent inhibition contributes to the level of viral inhibition achieved by a drug or drug combination following drug addition but that the stage at which a drug acts is not the sole determinant of its antiviral activity.

A limitation of our work is also that infections were performed by using a representative first-phase but not a second-phase cell type. Although the mathematical model can be used to analyze stage-dependent inhibition in first- or second-phase cell types separately (33), additional *in vitro* data obtained with a second-phase cell type, potentially a monocyte-derived macrophage culture, would prove valuable. A potential factor that might have affected our determination of the stage-dependent antiviral activity of entry inhibitors is that the direct cell-to-cell transfer of virus occurs with a much greater efficiency than cell-free infection in both cell lines and *in vivo*. Data as to whether direct cell-to-cell transfer might shield viral particles from the effects of entry inhibitors are inconclusive (24).

How exactly can stage-dependent inhibition account for the unique aspects of second-phase decay that were observed clinically with RAL? Notably, the rate of viral load decay during the second phase was observed to be the same with both EFV and RAL, but the level of viral RNA at the start of the second phase was 70% lower with RAL (26). It can be assumed that virus in this phase is produced by cells of the monocyte/macrophage lineage (2, 5, 34) that were infected before treatment began. Since infected macrophages appear to be resistant to immune-mediated clearance and die at the same rate, regardless of infection status, the rate of viral load decay in the second phase would not be expected to differ, no matter which drugs are used. The lower viral load at the start of the second phase with RAL is likely a result of the delayed kinetics of reverse transcription and integration during infection of monocytes and macrophages (3, 9, 18, 39, 41). The relatively long lag time between these two processes (up to 5 days in monocytes [3]) may give RAL a greater number of target cells in which to act compared to that for EFV when treatment begins. Thus, the additional viral load present at the start of the second phase with EFV but not RAL may arise from long-lived infected cells whose viruses had completed reverse transcription but not integration at the time that treatment began.

ACKNOWLEDGMENTS

REFERENCES

1. **Adachi, A., H. E. Gendelman, S. Koenig, T. Folks, R. Willey, A. Rabson, and M. A. Martin.** 1986. Production of acquired immunodeficiency syndrome-associated retrovirus in human and nonhuman cells transfected with an infectious molecular clone. J. Virol. **59:**284–291.
2. **Alexaki, A., Y. J. Liu, and B. Wigdahl.** 2008. Cellular reservoirs of HIV-1 and their role in viral persistence. Curr. HIV Res. **6:**388–400.
3. **Arfi, V., L. Riviere, L. Jarrosson-Wuilleme, C. Goujon, D. Rigal, J. L. Darlix, and A. Cimarelli.** 2008. Characterization of the early steps of infection of primary blood monocytes by human immunodeficiency virus type 1. J. Virol. **82:**6557–6565.
4. **Arnaout, R. A., M. A. Nowak, and D. Wodarz.** 2000. HIV-1 dynamics revisited: biphasic decay by cytotoxic T lymphocyte killing? Proc. Biol. Sci. **267:**1347–1354.
5. **Blankson, J. N., D. Persaud, and R. F. Siliciano.** 2002. The challenge of viral reservoirs in HIV-1 infection. Annu. Rev. Med. **53:**557–593.
6. **Cavert, W., D. W. Notermans, K. Staskus, S. W. Wietgrefe, M. Zupancic, K. Gebhard, K. Henry, Z. Q. Zhang, R. Mills, H. McDade, C. M. Schuwirth, J. Goudsmit, S. A. Danner, and A. T. Haase.** 1997. Kinetics of response in lymphoid tissues to antiretroviral therapy of HIV-1 infection. Science **276:**960–964.
7. **Chun, T. W., J. S. Justement, S. Moir, C. W. Hallahan, J. Maenza, J. I. Mullins, A. C. Collier, L. Corey, and A. S. Fauci.** 2007. Decay of the HIV reservoir in patients receiving antiretroviral therapy for extended periods: implications for eradication of virus. J. Infect. Dis. **195:**1762–1764.
8. **Chun, T. W., D. C. Nickle, J. S. Justement, D. Large, A. Semerjian, M. E. Curlin, M. A. O'Shea, C. W. Hallahan, M. Daucher, D. J. Ward, S. Moir, J. I. Mullins, C. Kovacs, and A. S. Fauci.** 2005. HIV-infected individuals receiving effective antiviral therapy for extended periods of time continually replenish their viral reservoir. J. Clin. Invest. **115:**3250–3255.
9. **Coleman, C. M., and L. Wu.** 2009. HIV interactions with monocytes and dendritic cells: viral latency and reservoirs. Retrovirology **6:**51.
10. **Dinoso, J. B., S. Y. Kim, A. M. Wiegand, S. E. Palmer, S. J. Gange, L. Cranmer, A. O'Shea, M. Callender, A. Spivak, T. Brennan, M. F. Kearney, M. A. Proschan, J. M. Mican, C. A. Rehm, J. M. Coffin, J. W. Mellors, R. F. Siliciano, and F. Maldarelli.** 2009. Treatment intensification does not reduce residual HIV-1 viremia in patients on highly active antiretroviral therapy. Proc. Natl. Acad. Sci. U. S. A. **106:**9403–9408.
11. **Finzi, D., J. Blankson, J. D. Siliciano, J. B. Margolick, K. Chadwick, T. Pierson, K. Smith, J. Lisziewicz, F. Lori, C. Flexner, T. C. Quinn, R. E. Chaisson, E. Rosenberg, B. Walker, S. Gange, J. Gallant, and R. F. Siliciano.** 1999. Latent infection of CD4+ T cells provides a mechanism for lifelong persistence of HIV-1, even in patients on effective combination therapy. Nat. Med. **5:**512–517.
12. **Finzi, D., and R. F. Siliciano.** 1998. Viral dynamics in HIV-1 infection. Cell **93:**665–671.
13. **Freed, E. O., G. Englund, and M. A. Martin.** 1995. Role of the basic domain of human immunodeficiency virus type 1 matrix in macrophage infection. J. Virol. **69:**3949–3954.
14. **Frenkel, L. M., Y. Wang, G. H. Learn, J. L. McKernan, G. M. Ellis, K. M. Mohan, S. E. Holte, S. M. De Vange, D. M. Pawluk, A. J. Melvin, P. F. Lewis, L. M. Heath, I. A. Beck, M. Mahalanabis, W. E. Naugler, N. H. Tobin, and J. I. Mullins.** 2003. Multiple viral genetic analyses detect low-level human immunodeficiency virus type 1 replication during effective highly active antiretroviral therapy. J. Virol. **77:**5721–5730.
15. **Goffinet, C., I. Allespach, L. Oberbremer, P. L. Golden, S. A. Foster, B. A. Johns, J. G. Weatherhead, S. J. Novick, K. E. Chiswell, E. P. Garvey, and O. T. Keppler.** 2009. Pharmacovirological impact of an integrase inhibitor on human immunodeficiency virus type 1 cDNA species in vivo. J. Virol. **83:**7706–7717.
16. **Hammer, S. M., J. J. Eron, Jr., P. Reiss, R. T. Schooley, M. A. Thompson, S. Walmsley, P. Cahn, M. A. Fischl, J. M. Gatell, M. S. Hirsch, D. M. Jacobsen, J. S. Montaner, D. D. Richman, P. G. Yeni, and P. A. Volberding.** 2008. Antiretroviral treatment of adult HIV infection: 2008 recommendations of the International AIDS Society—USA panel. JAMA **300:**555–570.
17. **Hlavacek, W. S., N. I. Stilianakis, D. W. Notermans, S. A. Danner, and A. S. Perelson.** 2000. Influence of follicular dendritic cells on decay of HIV during antiretroviral therapy. Proc. Natl. Acad. Sci. U. S. A. **97:**10966–10971.
18. **Kelly, J., M. H. Beddall, D. Yu, S. R. Iyer, J. W. Marsh, and Y. Wu.** 2008. Human macrophages support persistent transcription from unintegrated HIV-1 DNA. Virology **372:**300–312.
19. **Koelsch, K. K., L. Liu, R. Haubrich, S. May, D. Havlir, H. F. Gunthard, C. C. Ignacio, P. Campos-Soto, S. J. Little, R. Shafer, G. K. Robbins, R. T. D'Aquila, Y. Kawano, K. Young, P. Dao, C. A. Spina, D. D. Richman, and J. K. Wong.** 2008. Dynamics of total, linear nonintegrated, and integrated HIV-1 DNA in vivo and in vitro. J. Infect. Dis. **197:**411–419.

20. **Lennox, J. L., E. Dejesus, A. Lazzarin, R. B. Pollard, J. V. Madruga, D. S. Berger, J. Zhao, X. Xu, A. Williams-Diaz, A. J. Rodgers, R. J. Barnard, M. D. Miller, M. J. Dinubile, B. Y. Nguyen, R. Leavitt, and P. Sklar.** 2009. Safety and efficacy of raltegravir-based versus efavirenz-based combination therapy in treatment-naive patients with HIV-1 infection: a multicentre, double-blind randomised controlled trial. Lancet **374:**796–806.

21. **Lusso, P., F. Cocchi, C. Balotta, P. D. Markham, A. Louie, P. Farci, R. Pal, R. C. Gallo, and M. S. Reitz, Jr.** 1995. Growth of macrophage-tropic and primary human immunodeficiency virus type 1 (HIV-1) isolates in a unique CD4$^+$ T-cell clone (PM1): failure to downregulate CD4 and to interfere with cell-line-tropic HIV-1. J. Virol. **69:**3712–3720.

22. **Markowitz, M., B. Y. Nguyen, E. Gotuzzo, F. Mendo, W. Ratanasuwan, C. Kovacs, G. Prada, J. O. Morales-Ramirez, C. S. Crumpacker, R. D. Isaacs, H. Campbell, K. M. Strohmaier, H. Wan, R. M. Danovich, and H. Teppler.** Sustained antiretroviral effect of raltegravir after 96 weeks of combination therapy in treatment-naive patients with HIV-1 infection. J. Acquir. Immune Defic. Syndr. **52:**350–356.

23. **Markowitz, M., B. Y. Nguyen, E. Gotuzzo, F. Mendo, W. Ratanasuwan, C. Kovacs, G. Prada, J. O. Morales-Ramirez, C. S. Crumpacker, R. D. Isaacs, L. R. Gilde, H. Wan, M. D. Miller, L. A. Wenning, and H. Teppler.** 2007. Rapid and durable antiretroviral effect of the HIV-1 integrase inhibitor raltegravir as part of combination therapy in treatment-naive patients with HIV-1 infection: results of a 48-week controlled study. J. Acquir. Immune Defic. Syndr. **46:**125–133.

24. **Martin, N., and Q. Sattentau.** 2009. Cell-to-cell HIV-1 spread and its implications for immune evasion. Curr. Opin. HIV AIDS **4:**143–149.

25. **Munk, C., S. M. Brandt, G. Lucero, and N. R. Landau.** 2002. A dominant block to HIV-1 replication at reverse transcription in simian cells. Proc. Natl. Acad. Sci. U. S. A. **99:**13843–13848.

26. **Murray, J. M., S. Emery, A. D. Kelleher, M. Law, J. Chen, D. J. Hazuda, B. Y. Nguyen, H. Teppler, and D. A. Cooper.** 2007. Antiretroviral therapy with the integrase inhibitor raltegravir alters decay kinetics of HIV, significantly reducing the second phase. AIDS **21:**2315–2321.

27. **O'Doherty, U., W. J. Swiggard, and M. H. Malim.** 2000. Human immunodeficiency virus type 1 spinoculation enhances infection through virus binding. J. Virol. **74:**10074–10080.

28. **Perelson, A. S., P. Essunger, Y. Cao, M. Vesanen, A. Hurley, K. Saksela, M. Markowitz, and D. D. Ho.** 1997. Decay characteristics of HIV-1-infected compartments during combination therapy. Nature **387:**188–191.

29. **Perelson, A. S., A. U. Neumann, M. Markowitz, J. M. Leonard, and D. D. Ho.** 1996. HIV-1 dynamics in vivo: virion clearance rate, infected cell life-span, and viral generation time. Science **271:**1582–1586.

30. **Petitjean, G., Y. Al Tabaa, E. Tuaillon, V. Baillat, J. Reynes, M. Segondy, and J. P. Vendrell.** 2007. Unintegrated HIV-1 provides an inducible and functional reservoir in untreated and highly active antiretroviral therapy-treated patients. Retrovirology **4:**60.

31. **Pierson, T. C., Y. Zhou, T. L. Kieffer, C. T. Ruff, C. Buck, and R. F. Siliciano.** 2002. Molecular characterization of preintegration latency in human immunodeficiency virus type 1 infection. J. Virol. **76:**8518–8531.

32. **Ramratnam, B., R. Ribeiro, T. He, C. Chung, V. Simon, J. Vanderhoeven, A. Hurley, L. Zhang, A. S. Perelson, D. D. Ho, and M. Markowitz.** 2004. Intensification of antiretroviral therapy accelerates the decay of the HIV-1 latent reservoir and decreases, but does not eliminate, ongoing virus replication. J. Acquir. Immune Defic. Syndr. **35:**33–37.

33. **Sedaghat, A. R., J. B. Dinoso, L. Shen, C. O. Wilke, and R. F. Siliciano.** 2008. Decay dynamics of HIV-1 depend on the inhibited stages of the viral life cycle. Proc. Natl. Acad. Sci. U. S. A. **105:**4832–4837.

34. **Sedaghat, A. R., R. F. Siliciano, and C. O. Wilke.** 2009. Constraints on the dominant mechanism for HIV viral dynamics in patients on raltegravir. Antivir. Ther. **14:**263–271.

35. **Sedaghat, A. R., R. F. Siliciano, and C. O. Wilke.** 2008. Low-level HIV-1 replication and the dynamics of the resting CD4$^+$ T cell reservoir for HIV-1 in the setting of HAART. BMC Infect. Dis. **8:**2.

36. **Shen, L., S. Peterson, A. R. Sedaghat, M. A. McMahon, M. Callender, H. Zhang, Y. Zhou, E. Pitt, K. S. Anderson, E. P. Acosta, and R. F. Siliciano.** 2008. Dose-response curve slope sets class-specific limits on inhibitory potential of anti-HIV drugs. Nat. Med. **14:**762–766.

37. **Shen, L., and R. F. Siliciano.** 2008. Viral reservoirs, residual viremia, and the potential of highly active antiretroviral therapy to eradicate HIV infection. J. Allergy Clin. Immunol. **122:**22–28.

38. **Smith, S. D., M. Shatsky, P. S. Cohen, R. Warnke, M. P. Link, and B. E. Glader.** 1984. Monoclonal antibody and enzymatic profiles of human malignant T-lymphoid cells and derived cell lines. Cancer Res. **44:**5657–5660.

39. **Sonza, S., A. Maerz, N. Deacon, J. Meanger, J. Mills, and S. Crowe.** 1996. Human immunodeficiency virus type 1 replication is blocked prior to reverse transcription and integration in freshly isolated peripheral blood monocytes. J. Virol. **70:**3863–3869.

40. **Strain, M. C., H. F. Gunthard, D. V. Havlir, C. C. Ignacio, D. M. Smith, A. J. Leigh-Brown, T. R. Macaranas, R. Y. Lam, O. A. Daly, M. Fischer, M. Opravil, H. Levine, L. Bacheler, C. A. Spina, D. D. Richman, and J. K. Wong.** 2003. Heterogeneous clearance rates of long-lived lymphocytes infected with HIV: intrinsic stability predicts lifelong persistence. Proc. Natl. Acad. Sci. U. S. A. **100:**4819–4824.

41. **Triques, K., and M. Stevenson.** 2004. Characterization of restrictions to human immunodeficiency virus type 1 infection of monocytes. J. Virol. **78:**5523–5527.

42. **Yamamoto, N., C. Tanaka, Y. Wu, M. O. Chang, Y. Inagaki, Y. Saito, T. Naito, H. Ogasawara, I. Sekigawa, and Y. Hayashida.** 2006. Analysis of human immunodeficiency virus type 1 integration by using a specific, sensitive and quantitative assay based on real-time polymerase chain reaction. Virus Genes **32:**105–113.

43. **Yu, J. J., T. L. Wu, M. K. Liszewski, J. Dai, W. J. Swiggard, C. Baytop, I. Frank, B. L. Levine, Y. Yang, T. Theodosopoulos, and U. O'Doherty.** 2008. A more precise HIV integration assay designed to detect small differences finds lower levels of integrated DNA in HAART treated patients. Virology **379:**78–86.

44. **Zhang, H., Y. Zhou, C. Alcock, T. Kiefer, D. Monie, J. Siliciano, Q. Li, P. Pham, J. Cofrancesco, D. Persaud, and R. F. Siliciano.** 2004. Novel single-cell-level phenotypic assay for residual drug susceptibility and reduced replication capacity of drug-resistant human immunodeficiency virus type 1. J. Virol. **78:**1718–1729.

45. **Zhou, Y., H. Zhang, J. D. Siliciano, and R. F. Siliciano.** 2005. Kinetics of human immunodeficiency virus type 1 decay following entry into resting CD4$^+$ T cells. J. Virol. **79:**2199–2210.